World Journal of Advanced Research and Reviews
eISSN: 2581-9615 CODEN (USA): WJARAI
Cross Ref DOI: 10.30574/wjarr
Journal homepage: https://wjarr.com/

(RESEARCH ARTICLE)

Check for updates

Research on deformation control of thin-walled parts with support force and milling parameters based on mirror milling system

Yantong Gong [1, 2, *] and Xiaobin Liu [1, 2]

[1] *School of Mechanical Engineering, Tianjin University of Technology and Education, Tianjin 300222*
[2] *Tianjin Key Laboratory of Intelligent Robot Technology and Applications, Tianjin 300222*

World Journal of Advanced Research and Reviews, 2026, 30(03), 862-869

Publication history: Received on 27 April 2026; revised on 01 June 2026; accepted on 03 June 2026

Article DOI: https://doi.org/10.30574/wjarr.2026.30.3.1607

Abstract

Aiming at the severe machining deformation of aerospace aluminum alloy thin-walled parts during mirror milling, the coupled influence mechanism of support force and milling parameters on workpiece deformation is investigated based on the finite element software ABAQUS. A finite element model of the mirror milling system is established to analyze the variation law of thin-walled part deformation affected by support force as well as its interaction with milling parameters. On this basis, a numerical simulation model for the milling process is constructed, and workpiece deformation data corresponding to the parameter combination with maximum local stiffness of the workpiece are obtained systematically by orthogonal experimental design. Experimental verification demonstrates that the predicted deformation from simulation agrees well with measured experimental data, with the minimum relative error of 4.38% and the maximum relative error of 9.35%. The research indicates that the parameter optimization method combining finite element simulation and intelligent algorithm can effectively suppress the machining deformation of aerospace thin-walled components and improve their forming quality.

Keywords: Thin-walled parts; support force; Milling parameters; ABAQUS; Deformation control

1. Introduction

In the aerospace industry, thin-walled components serve as critical structural parts featuring light weight and high specific strength. Nevertheless, such components are generally characterized by large outline dimensions and small wall thickness, resulting in low inherent stiffness and severe deformation problems during machining. As an emerging advanced machining technology developed in recent years, mirror milling arranges the supporting head and cutting tool in a mirrored layout to realize synchronous movement. Its core advantage lies in providing real-time local follow-up support for workpieces, which improves the rigidity of the machining system, suppresses cutting vibration and reduces final machining deformation. In this process, collaborative optimization of support force and milling parameters is crucial for deformation control. At present, process parameter selection in practical production mostly relies on empirical judgment, which lacks systematic theoretical guidance, leads to unstable machining quality and excessive tool wear, and fails to guarantee the dimensional accuracy of finished components.

Ma et al. [1] established a finite element (FE) simulation model for thin-walled parts to analyze the effects of varying support force and milling parameters on machining deformation, and verified that optimizing the magnitude and layout of support force can effectively reduce vibration and deformation during cutting. Wu Hongbing [2] conducted in-depth research on key FE simulation technologies and constructed the FE model of integral frame parts, revealing that symmetric milling can greatly reduce machining deformation. Briceno et al. [3] compared the performance of back propagation neural network (BPNN) and radial basis neural network (RBNN) in end-milling force prediction and

* Corresponding author: Yantong Gong

selected the more efficient and accurate network for milling process modeling. Zhang Xinyun et al. [4] adopted ABAQUS to investigate the deformation of aerospace frame thin-walled parts induced by clamping scheme and milling parameters, and optimized clamping positions and cutting parameters by combining BP neural network with genetic algorithm; experimental results proved that optimized parameters can significantly improve machining quality. Patru et al. [5] analyzed the aluminum alloy milling process via finite element method and supplied abundant numerical data for exploring the mechanical characteristics in cutting.

In summary, finite element simulation is an effective tool for analyzing cutting deformation of thin-walled parts and provides solid technical support for deformation control [6]. However, existing researches mainly concentrate on conventional milling and only optimize cutting parameters separately, rarely focusing on the mirror milling process. Most studies ignore the influence of support force as well as its coupling effect with milling parameters, hence existing research conclusions cannot be directly applied to the practical mirror milling of aerospace aluminum alloy thin-walled components.

To fill the above research gaps, this paper takes aerospace aluminum alloy thin-walled parts as research objects and systematically investigates the coupled effect of support force and milling parameters on machining deformation based on finite element simulation. Furthermore, practical cutting experiments are carried out with the optimal parameter combinations obtained from simulation to verify the effectiveness and reliability of the proposed parameter matching strategy in reducing mirror milling deformation.

1.1. Deformation of Thin-Walled Workpiece under Variable Support Force in Mirror Milling

The application of support force is critical to guarantee machining precision during mirror milling. Appropriate support force can improve the structural stiffness of thin-walled parts to resist cutting loads and machining vibration, so as to enhance machining stability. Excessively large support force, however, may trigger excessive deformation and regenerative chatter of the workpiece [8]. Accordingly, reasonable configuration of support force is essential for deformation suppression of thin-walled components.

1.1.1. Modal Hammering Test

Variable support forces ranging from 0 N to 400 N are loaded by regulating the servo motor of the support head. The supporting and excitation positions coincide at the central region of the workpiece, while the vibration pickup point is arranged on the opposite side of the thin-walled specimen as shown in Fig.1. Four discrete support levels of 0 N, 100 N, 200 N, 300 N and 400 N are applied at the central position for modal hammer excitation tests. Each excitation test is repeated three times and the average value is taken as measured data. By comparing the frequency response functions (FRFs) under various support loads, the influence of variable support force on the dynamic characteristics of thin-walled parts is characterized.

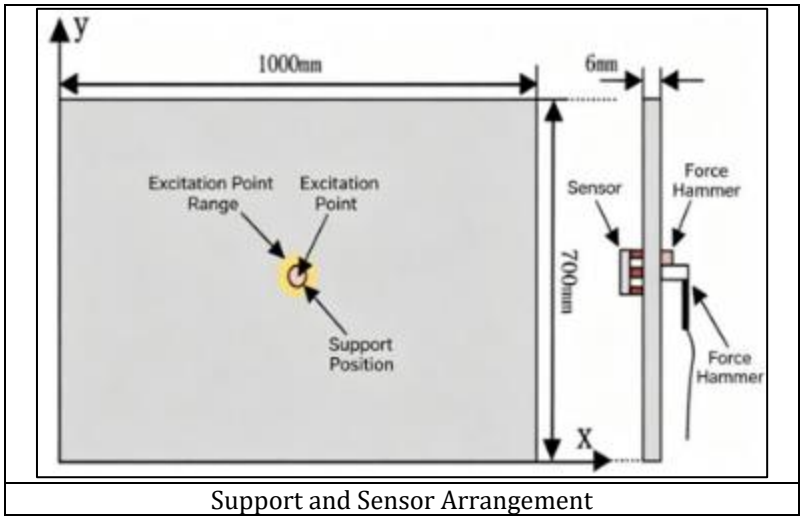

Figure 1 Layout of Supports and Sensors for Modal Hammer Test

After the above tests, all frequency response functions under different support forces are exported via DASP software. The orthogonal polynomial identification method is adopted to fit and calculate modal parameters including natural frequency and damping ratio, as listed in Table 1.

Table 1 Modal Parameters under Different Support Forces

Support force/N	Modal parameters	1st order	2nd order	3rd order
0	Frequency/Hz	89.2	106.7	170.4
	Damping ratio%	0.0055	0.0067	0.0032
100	Frequency/Hz	92.3	108.1	176.9
	Damping ratio%	0.0244	0.0114	0.0087
200	Frequency/Hz	100.4	118.2	186.3
	Damping ratio%	0.0278	0.0191	0.0090
300	Frequency/Hz	108.4	138.9	200.3
	Damping ratio%	0.0265	0.0131	0.0055
400	Frequency/Hz	119.2	159.5	239.6
	Damping ratio%	0.0208	0.0135	0.0051

When the support force is 0 N, the damping ratios are low (0.0055 for the 1st order, 0.0067 for the 2nd order and 0.0032 for the 3rd order), indicating low vibration energy dissipation, high susceptibility to intense vibration and poor system stability. With rising support force, the damping ratios increase gradually and reach 0.0278 (1st), 0.0191 (2nd) and 0.0090 (3rd) at 200 N. At this load, the system dissipates vibration energy efficiently and suppresses unwanted vibration effectively. Further increasing the support force leads to a slight decline and stabilization of damping ratios, meaning the vibration suppression effect becomes saturated. The 200 N support force optimizes the structural damping dominated by interfacial friction while greatly improving structural stiffness, avoiding nonlinear problems such as damping degradation and modal jump induced by excessive constraint.

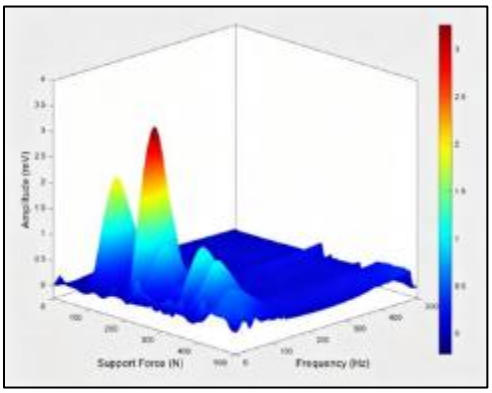

Figure 2 Fitting of Frequency Response Functions under Support Forces from 0 N to 400 N

As shown in the 3D surface plot of frequency response functions in Figure 2, the support force of 200 N achieves the optimal suppression of resonant response and keeps the amplitude low across the full frequency range. A sensitive resonant band exists between 150 Hz and 300 Hz. When the support force is below 200 N, obvious amplitude peaks appear within this band, implying high vibration risk. Increasing the support force to 200 N eliminates all high-amplitude regions in the resonant band, and the frequency response amplitude remains low over the entire frequency domain. It demonstrates that 200 N effectively restrains severe resonant vibration and ensures stable performance in the non-resonant range of 300–400 Hz.A distinct threshold effect is observed between support force and response amplitude. As the support force rises from 0 N to 200 N, resonant peak amplitude drops rapidly; beyond 200 N, the amplitude barely decreases further and the vibration suppression effect becomes saturated. Therefore, 200 N is the critical saturation value for vibration reduction. The first four modal shapes under 200 N are presented in Figure 3.

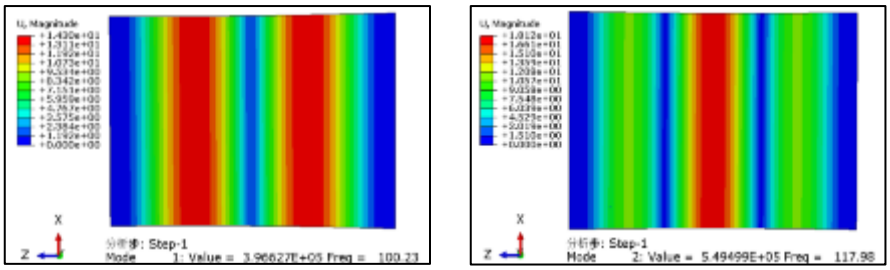

(a)1st-order modal shape (b)2nd-order modal shape

(c)3rd-order modal shape (d)4th-order modal shape

Figure 3 First Four Orders of Modal Shapes under 200 N Support Force

1.2. Finite Element Simulation on Milling of Thin-Walled Parts

1.2.1. Establishment of Finite Element Model

The three-dimensional geometric model of the mirror milling system for thin-walled components is constructed via SolidWorks and subsequently imported into ABAQUS finite element software. Table 2 lists the chemical composition of 2A12 aerospace aluminum alloy [7], and Table 3 summarizes cutter parameters. The workpiece is made of 2A12 aluminum alloy with dimensions of 1000×700×6 mm and curvature radius of 4000 mm. Its material properties are specified as: density 2640 kg/m^3, Young's modulus 69.35 GPa、6.8×10^{10} Pa, Poisson's ratio 0.3. Assigning accurate material parameters in the preprocessing stage of ABAQUS is essential to guarantee calculation reliability, and the constituent proportions of 2A12 are tabulated in Table 2.

A three-flute cemented carbide end mill is adopted in this work, with key geometric parameters: diameter 10 mm, rake angle 8°, clearance angle 9°, helix angle 35°, as detailed in Table 3. To realize reliable positioning of the thin-walled workpiece, a symmetric clamping scheme with ten clamping points on each left and right side is adopted. Since the influence of milling trajectory on workpiece deformation is excluded from this study, only the condition with central supporting position is simulated. Tetrahedral elements are employed for global meshing; local mesh refinement is performed along the milling path to improve computational precision. Fixed constraints are applied on both lateral sides (see Fig.4). Deformation simulations under various working conditions are realized by adjusting the magnitude of support force.

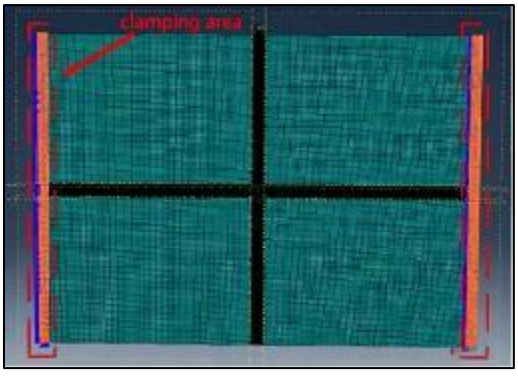

Figure 4 Mesh Generation of Milling System

Table 2 Chemical Composition of 2A12 Aerospace Aluminum Alloy

Chemical composition	Si	Cu	Mg	Zn	Mn	Ti	Ni	Fe
Content (%)	≤0.50	3.8~4.9	1.2~1.8	≤0.30	0.30~0.9	≤0.15	≤0.10	0~0.50

Table 3 Cutting Tool Parameters

Name	Material Property	Young's Modulus	Poisson's Ratio	Density	Dimension
Cutting tool	Cemented carbide	4.5e11Pa	0.25	14500kg/m3	-

1.3. Three-Dimensional Finite Element Simulation of Milling

To investigate the influence of milling parameters on the machining deformation of thin-walled parts, this work concentrates on the rough milling stage, and the established 3D finite element milling model is displayed in Figure 5. Since improving material removal efficiency is the primary objective in rough milling, a relatively large cutting width is commonly adopted. Accordingly, the cutting width is fixed in this study and excluded from variable analysis, while three critical parameters, namely spindle speed, axial cutting depth and feed rate, are selected as research objects.

An orthogonal experiment with three factors and four levels is designed as listed in Table 4. Three-dimensional finite element milling simulations are implemented to calculate workpiece deformation under various parameter combinations, and the corresponding deformation values are finally obtained.

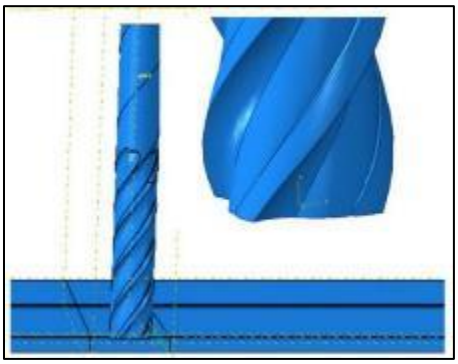

Figure 5 Three-dimensional Finite Element Simulation Model

Table 4 Deformation of Thin-walled Parts

No.	Support Force（N）	Spindle Speed n(rpm)	Axial Depth of Cut a_p(mm)	Feed Speed v_f(mm/min)	Deformation/μm
1	100	4000	0.1	288	14
2	200	4000	0.5	360	23
3	300	4000	1.0	288	16
4	400	4000	1.5	360	21
5	100	6000	0.1	288	25
6	200	6000	0.5	360	18
7	300	6000	1.0	288	22
8	400	6000	1.5	360	21
9	100	8000	0.1	288	19
10	200	8000	0.5	360	23

11	300	8000	1.0	288	27
12	400	8000	1.5	360	15

1.4. Experimental Verification

The experiment is carried out on a mirror milling system dedicated to large-scale thin-walled components, as illustrated in Figure 6.

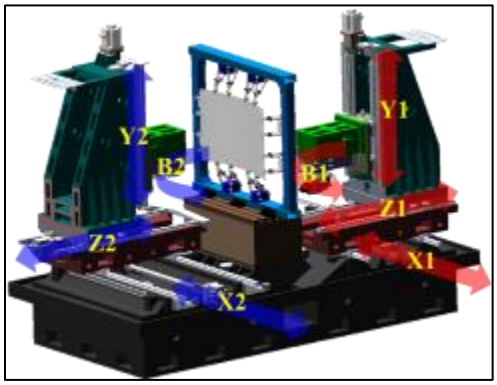

Figure 6 Schematic Diagram of Mirror Milling for Thin-Walled Parts

Practical mirror milling tests are performed to verify the accuracy of the optimized results. After machining, a coordinate measuring machine (CMM, shown in Figure 7) is adopted. Ten measuring points with equal spacing are selected at the middle region of the workpiece bottom surface to measure the positional deviation along the Z-axis, from which the Z-direction deformation at corresponding sampling points is acquired. The experimental results are presented in Figure 8.

(a)Vertical MC (b)CMM

Figure 7 Experimental Equipment

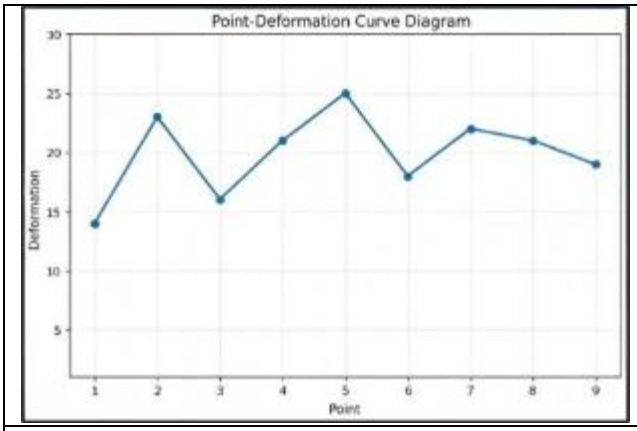

(a)Predicted deformation

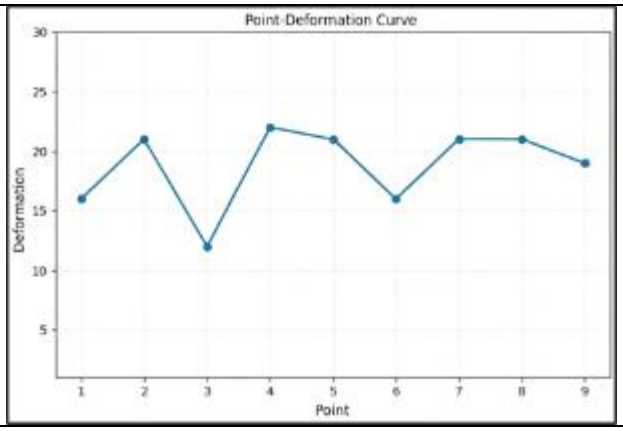

(b)Measured deformation

Figure 8 Comparison Diagram of Deformation

By comparing the curves of predicted deformation in Figure (a) and measured experimental deformation in Figure (b), it can be found that the variation trend of predicted deformation at nine measuring points is highly consistent with the law of experimental measured deformation. Both curves rise from Point 1 and reach the first peak at Point 2, fall to the minimum deformation of the whole curve at Point 3, and rebound to a local maximum at Point 4. Afterwards, the deformation fluctuates slightly and declines slowly from Point 5 to Point 9, with completely coincident positions of peaks and valleys. It demonstrates that the established simulation model can accurately reproduce the practical deformation evolution characteristics of the workpiece. In terms of numerical values, the deviations between predicted and measured deformation at all points are within a reasonable range without abrupt magnitude changes, and only minor numerical differences exist at partial measuring points. The above results verify the rationality of material parameters, boundary constraints and loading conditions adopted in simulation modeling, proving favorable reliability of the model. In conclusion, the proposed simulation method can effectively predict workpiece deformation, which supports pre-analysis of deformation under various process parameters and further optimization of machining schemes to reduce finished-product deformation error in advance.

2. Conclusions

Taking mirror milling of thin-walled workpieces made of 2A12 aerospace aluminum alloy as the research object, this paper aims to solve the problem of easy machining deformation caused by low rigidity of thin-walled components. Combining hammer modal test, ABAQUS finite element simulation and practical milling experiment, the coupling effects of support force, spindle speed, axial depth of cut and feed speed on workpiece machining deformation are systematically investigated. This research remedies the deficiency of existing studies that mostly ignore the effect of follow-up support in mirror milling and only optimize cutting parameters separately. The main conclusions are summarized as follows:

Support force presents an obvious threshold effect on dynamic characteristics and vibration suppression performance of thin-walled parts. As the support force increases from 0 N to 200 N, the natural frequencies of each order rise continuously and the system damping ratio increases remarkably with drastically reduced vibration amplitude within resonant frequency bands. The optimal critical support force is 200 N, at which the interfacial frictional damping works sufficiently to suppress vibration in the sensitive resonant range of 150–300 Hz. Further increase of support force leads to slight damping reduction and saturated vibration damping effect; excessive support force tends to induce extra local extrusion deformation of the workpiece.

Among milling process parameters, axial depth of cut dominates machining deformation. According to orthogonal simulation experiments with three factors and four levels, increased axial depth of cut brings larger cutting load and aggravates elastic deformation of the workpiece. Spindle speed and feed speed adjust chatter initiation probability by altering milling excitation frequency, and mismatched parameter configuration will trigger sharp rise of local deformation. Under the optimal support force of 200 N, most deformation increment induced by cutting load can be counteracted, forming the critical matching condition for deformation control.

Compliance with ethical standards

Disclosure of conflict of interest

No conflict of interest to be disclosed.

References

[1] Ma L, Ba S, Zhang Y, et al. Prediction of Milling Deformation for Frame-Type Thin-Walled Parts Considering Workblank Initial Residual Stress and Milling Force[J]. Journal of Manufacturing and Materials Processing, 2025, 9(5): 146.

[2] Wu H B. Numerical Simulation and Experimental Study on Milling Deformation of Integral Aerospace Frame Structural Parts[D]. Hangzhou: Zhejiang University, 2008.

[3] Briceno J F, El-Mounayri H, Mukhopadhyay S. Selecting an artificial neural network for efficient modeling and accurate simulation of the milling process[J]. International Journal of Machine Tools and Manufacture, 2002, 42(6): 663-674.

[4] Zhang X Y, Dong J, Cao Y, et al. Research on Clamping Layout and Machining Parameters of Frame Thin-Walled Parts[J]. Manufacturing Technology & Machine Tool, 2024(06):11-17. DOI:10.19287/j.mtmt.1005-2402.2024.06.002.

[5] Patru E N, Bica M, Craciunoiu N, et al. Analysis of Milling Process of Aluminum Alloy Using Finite Element Method[C]//Proceedings of the International Conference on Mechanical Engineering (ICOME 2022). Springer Nature, 2023, 15: 455.

[6] Dong J. Deformation Prediction and Parameter Optimization in Cutting of Aerospace Thin-walled Parts[D]. Xi'an: Xi'an Technological University, 2024. DOI:10.27391/d.cnki.gxagu.2024.000307.

[7] Wu H X. Research on Cryoforming Process of Conical Curved Parts of 2A12 Aluminum Alloy[D]. Dalian: Dalian University of Technology, 2025. DOI:10.26991/d.cnki.gdllu.2025.000710.

[8] Chen X W. Research on Chatter Monitoring and Suppression Method for Thin-Walled Cylinder during Robotic Milling[D]. Qinhuangdao: Yanshan University, 2025. DOI:10.27440/d.cnki.gysdu.2025.001856.